

## Measurement of the Nuclear Slope Parameter of the $p\bar{p}$ Elastic-Scattering Distribution at $\sqrt{s} = 1800$ GeV

N. A. Amos,<sup>(3)</sup> W. F. Baker,<sup>(4)</sup> M. Bertani,<sup>(1)</sup> M. M. Block,<sup>(7)</sup> R. DeSalvo,<sup>(3)</sup> D. A. Dimitroyannis,<sup>(6)</sup> A. Donati,<sup>(7)</sup> D. P. Eartly,<sup>(4)</sup> R. W. Ellsworth,<sup>(5)</sup> G. Giacomelli,<sup>(1)</sup> J. A. Goodman,<sup>(6)</sup> C. M. Guss,<sup>(7)</sup> A. J. Lennox,<sup>(4)</sup> R. Maleyran,<sup>(2)</sup> A. Manarin,<sup>(2)</sup> M. R. Mondardini,<sup>(1)</sup> J. P. Negret,<sup>(4)</sup> J. Orear,<sup>(3)</sup> S. M. Pruss,<sup>(4)</sup> R. Rubinstein,<sup>(4)</sup> S. Shukla,<sup>(7)</sup> G. B. Yodh,<sup>(6)</sup> T. York,<sup>(3)</sup> and S. Zucchelli<sup>(1)</sup>

(E710 Collaboration)

<sup>(1)</sup>Università di Bologna and Istituto Nazionale di Fisica Nucleare, Bologna, Italy

<sup>(2)</sup>CERN, Geneva, Switzerland

<sup>(3)</sup>Cornell University, Ithaca, New York 14853

<sup>(4)</sup>Fermi National Accelerator Laboratory, Batavia, Illinois 60510

<sup>(5)</sup>George Mason University, Fairfax, Virginia 22030

<sup>(6)</sup>University of Maryland, College Park, Maryland 20742

<sup>(7)</sup>Northwestern University, Evanston, Illinois 60201

(Received 18 March 1988)

We have studied proton-antiproton elastic scattering at  $\sqrt{s} = 1800$  GeV at the Fermilab Collider, in the range  $0.02 < |t| < 0.13$  (GeV/c)<sup>2</sup>. Fitting the distribution by  $\exp(-B|t|)$ , we obtain a value of  $B$  of  $17.2 \pm 1.3$  (GeV/c)<sup>-2</sup>.

PACS numbers: 13.85.Dz

Fermilab experiment E710 has as its main goals the measurement of  $\sigma_t$ , the proton-antiproton total nuclear cross section,  $B$ , the nuclear logarithmic slope parameter of the proton-antiproton elastic-scattering distribution, and  $\rho$ , the ratio of the real to imaginary part of the forward nuclear scattering amplitude, at energies from  $\sqrt{s}$  of 300 to 2000 GeV. Experiments measuring the  $p\bar{p}$  total cross section have shown that this quantity falls with increasing energy, reaches a minimum of about  $\sqrt{s} = 20$  GeV, and then rises as the energy is further increased. Similar behavior is observed for the  $pp$  total cross section. The slope parameter  $B$  is related to  $\sigma_t$  (for scattering from a black disk of radius  $R$ , for example,  $B$  is given by  $R^2/4$  and the total cross section by  $2\pi R^2$ ); at energies above  $\sqrt{s} = 20$  GeV,  $B$  increases with energy similarly to the total cross section. At present, there is no clear understanding of why  $\sigma_t$  or  $B$  should be increasing with energy, and whether they will continue to rise indefinitely or approach infinite values. Accurate measurements of  $\sigma_t$ ,  $B$ , and  $\rho$  at several energies, especially as new accelerators allow scattering at higher energies to be studied, will it is hoped lead to a theoretical understanding of these phenomena. We report here a measurement of  $B$  at  $\sqrt{s} = 1800$  GeV, using data taken in the first run of the Fermilab Tevatron Collider.

Previous measurements of this quantity above  $\sqrt{s} \sim 10$  GeV have been made at fixed-target accelerators,<sup>1,2</sup> the CERN ISR,<sup>3,4</sup> and the CERN SPS collider.<sup>5</sup> These earlier data show that the logarithmic slope  $B$  near  $t=0$  (where  $t$  is the square of the four-momentum transfer) increases with  $s$ , with values of  $B$  of about  $13$  (GeV/c)<sup>-2</sup>

at the ISR and rising to  $\sim 15$  (GeV/c)<sup>-2</sup> at the SPS collider. Similar measurements have been made for proton-proton scattering.<sup>1-4,6-9</sup>

A schematic view of the experiment layout is shown in Fig. 1. The experiment was located on both sides of the Tevatron E0 interaction point. Detectors for registering small-angle elastic scattering in the vertical plane were located in "Roman pots," thin-walled reentrant vessels which could be moved remotely, allowing the detectors

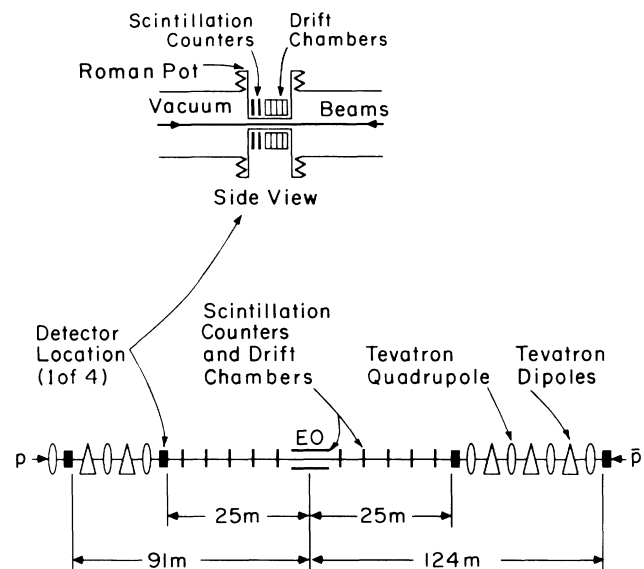


FIG. 1. Schematic view of the experiment layout.

to be placed close to the accelerator circulating beams. A precision motor and readout system allowed a repositioning accuracy of  $\sim 5 \mu\text{m}$ , and an absolute location accuracy of  $\sim 15 \mu\text{m}$ . These pots were symmetrically placed, one above and one below the circulating beam, making a pair. There were four such pairs, one each at the two ends of the 50-m E0 straight section ("inner pots") and the other two pairs ("outer pots") located in either direction about 100 m from E0 in the Tevatron lattice; special warm beam-pipe sections were made to allow installation of our pots at these latter positions in the superconducting accelerator. The beam optics were such that the effective distances to these latter detectors were about 80 m in the vertical plane and 40 m in the horizontal plane. The large effective distance in the vertical plane allowed detection of scattering at very small angles. Located around the E0 straight-section beam pipe were 48 scintillation counters and 32 small drift chambers used to measure the total inelastic counting rate.

The results to be presented here were obtained with use of the detectors in the outer pots. Each pot contained two scintillation counters (28 mm horizontally by 23 mm vertically) for triggering and a drift chamber.<sup>10</sup> Each drift chamber had four sense wires, giving four measurements of the vertical coordinates of a particle track by drift time and four measurements of horizontal coordinates by charge division. Elastic events were recorded by the triggering of the  $\bar{p}$ -arm upper detector in coincidence with the  $p$ -arm lower detector, and vice versa, although data were also taken with other combinations for background studies. Because of the  $\sim 100$  m of 4-T magnets between the interaction point and the pots, background rates were generally low.

Following the establishment of stable colliding beams in the accelerator, each pot was moved in toward the circulating beams, until the scintillators in the pot registered an abrupt increase in counting rate, as the edges of the beams were encountered. The pots were then backed off equally (about 1 mm) from this position. Thus, for data taking, the two pots of a pair were located symmetrically around the beam center (the beam center was assumed to be midway between the upper and lower beam edges). The closest distance achieved from beam center to the detector edge was 5 mm, corresponding to a minimum angle of about  $60 \mu\text{rad}$ . For most data taking, the detectors in the pots were placed with their closest edge about 10 mm from the beam center. In the data reported here, the detector acceptance was  $0.017 < |t| < 0.18$  ( $\text{GeV}/c$ )<sup>2</sup>, and we give results for the range  $0.02 < |t| < 0.13$  ( $\text{GeV}/c$ )<sup>2</sup>. The typical luminosity at our E0 intersection was  $\sim 5 \times 10^{26} \text{ cm}^{-2} \text{ s}^{-1}$ . Because of the high beta functions at E0 compared to B0 (where the CDF detector was located), our luminosity was about  $\frac{1}{80}$  of the B0 luminosity. Typical accelerator vertical beta functions were 0.7 m at B0, 53 m at E0, and 158

and 104 m at the outer detectors. Beam angular divergences at the E0 interaction point were  $\sim \pm 16 \mu\text{rad}$ .

In this first run we encountered some problems (which have now been corrected) that resulted in drift-chamber wires becoming coated with contaminants. This resulted in reduced wire efficiencies and degradation of charge-division resolution. For each run used in the analysis, we examined the efficiencies of the wires. We only used those wires that demonstrated high and reasonably uniform efficiency, and averaged the coordinates of the wires used to produce one  $(x,y)$  (horizontal, vertical) coordinate pair for the chamber for subsequent analysis. The number of wires used per chamber varied from one to three. As a consistency check, some runs were analyzed with use of other techniques (e.g., by the forming of tracks from the wire coordinates); the values of  $B$  obtained were always in agreement.

The following cuts, in this order, were used to define elastic candidates:

(1) Events were rejected if the appropriate scintillation counters in the pots did not have the correct time of flight for particles coming from the E0 interaction point.

(2) Events were rejected if any of the inelastic counters were struck with particles whose time of flight was consistent with their originating from a beam-beam interaction at the intersection region E0; this was also done if there were in-time counts in inner pot scintillators that could have been traversed by the elastically scattered particles.

(3) Events were rejected if there was the possibility of more than one track in any drift chamber.

We show in Fig. 2 (for a typical run) the correlation

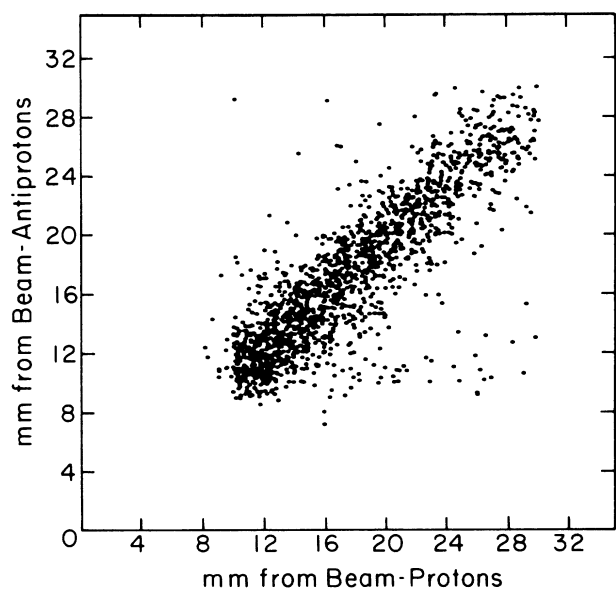


FIG. 2. Correlation for one run between the vertical coordinates of a corresponding pair of drift chambers, one on the proton side and one on the antiproton side.

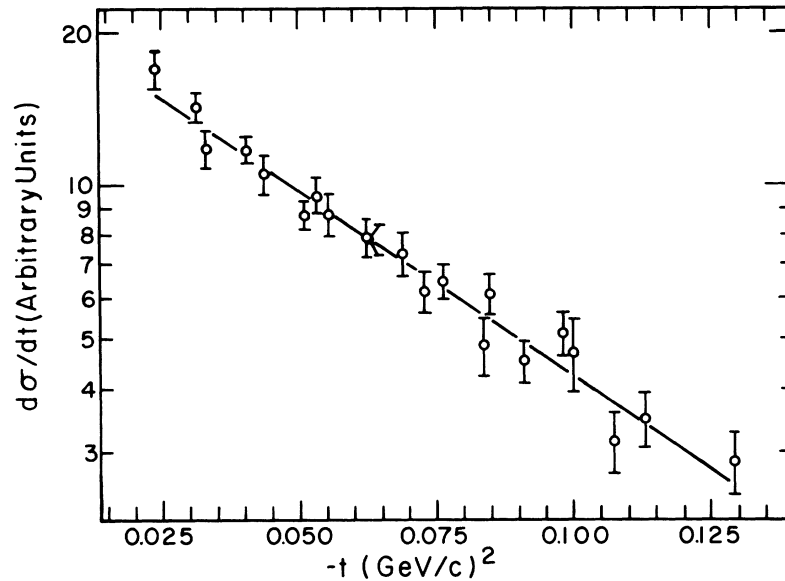


FIG. 3. Elastic-scattering distribution obtained for one run; the line shown is the fit described in the text.

between the vertical coordinates in a corresponding pair of chambers. As can be seen, almost all events cluster along the diagonal where elastic candidates should appear. The main contributions to the diagonal's width are due to the finite vertical beam size and vertical angular divergence of the colliding beams, with only a minor contribution arising from the vertical spatial resolution (drift time) of the drift chambers. A similar figure is obtained for the horizontal coordinates, but with a significantly larger width ( $\pm 3$  mm) because of the poor charge-division resolution mentioned above. Further

cuts were made in both variables to eliminate off-diagonal events; the remaining inelastic background under the elastic signal was small [ $\sim(2-3)\%$ ] and was corrected for.

The analysis procedure used to obtain the logarithmic slope of the elastic-scattering distribution is essentially identical to that used in a previous similar experiment.<sup>4,11,12</sup> This procedure takes into account smearing due to beam size and divergence, scattering position, drift-time resolution, and charge-division resolution in a self-consistent way. The parameters derived from the

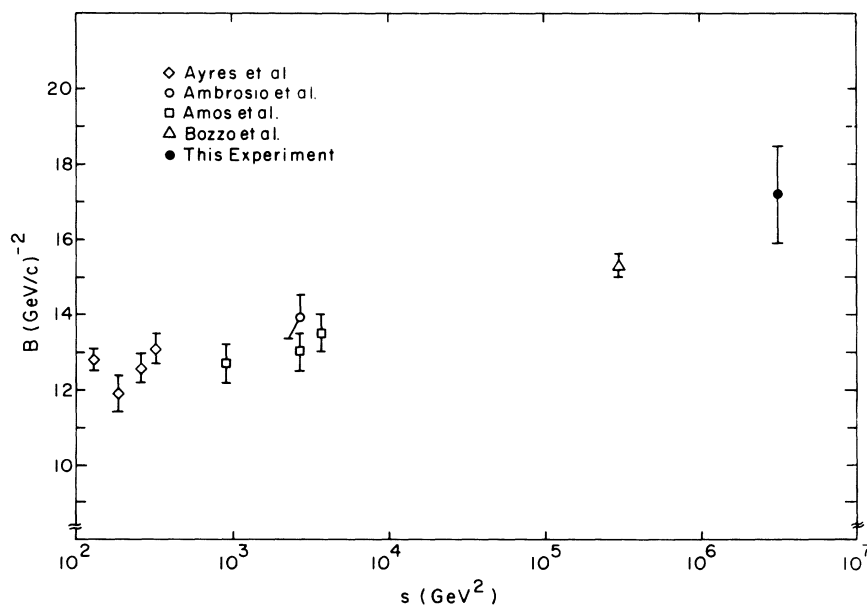


FIG. 4.  $B$  values obtained from this experiment, and previous  $\bar{p}p$  data (Refs. 1 and 3-5) for values of  $|t| \lesssim 0.1$  (GeV/c)<sup>2</sup>.

observed smearing are used to correct for events lost at the borders of the detectors.

The cross section  $d\sigma/dt$  consists of three terms: Coulomb, Coulomb-nuclear interference, and nuclear scattering.<sup>13,14</sup> In this present work, we have not attempted to derive an absolute normalization, and Coulomb effects are not significant in the range of  $t$  covered by our data. We thus fitted for only the logarithmic slope parameter  $B$ .

For this report, we have analyzed 3050 elastic events from five runs, each of which lasted a few hours. Events were binned in rectangles in the  $(x,y)$  chamber coordinates, and plotted at the average  $t$  value for each bin. In Fig. 3 we show the  $t$  distribution obtained from one of the runs, which contains 1934 elastic events. We have fitted the data of this run by the form  $d\sigma/dt = A \times \exp(-B|t|)$  and obtain  $B = 16.6 \pm 1.1$  (GeV/c)<sup>-2</sup>. We have verified that the  $B$  value and the  $\chi^2$  of the fit are stable under changes in the  $x$  and  $y$  regions of the drift chambers used to obtain the elastic events.

Data from all five runs are self-consistent, and we combine them to obtain our final value for  $B$  which is  $B = 17.2 \pm 0.9$  (statistical error). In this run, we estimate the systematic error in  $B$  to be  $\pm 1.0$  (GeV/c)<sup>-2</sup>; this is due to uncertainties in the effective distances to the detectors, uncertainties in the drift velocities in the chambers, and uncertainties in counter and chamber spatial efficiencies (all of which will be greatly reduced in future running). Our final result with combined error is  $B = 17.2 \pm 1.3$  (GeV/c)<sup>-2</sup>. This result is consistent with

reasonable extrapolations from lower-energy data as seen in Fig. 4, where we show data from this and previous experiments for  $|t| \lesssim 0.1$  (GeV/c)<sup>2</sup>.

We wish to thank the Fermilab Accelerator Division staff for much help in making these measurements possible, and CERN for assistance with the Roman pots and drift-chamber readout system. We gratefully acknowledge financial support from the U.S. Department of Energy, Contract No. DE-AC02-76-ER-02289 Task B, the U.S. National Science Foundation, the Italian Ministero Pubblica Istruzione (60%), and the North Atlantic Treaty Organization.

<sup>1</sup>D. S. Ayres *et al.*, Phys. Rev. D **15**, 3105 (1977).

<sup>2</sup>L. A. Fajardo *et al.*, Phys. Rev. D **24**, 46 (1981).

<sup>3</sup>M. Ambrosio *et al.*, Phys. Lett. **115B**, 495 (1982).

<sup>4</sup>N. Amos *et al.*, Nucl. Phys. **B262**, 689 (1985).

<sup>5</sup>M. Bozzo *et al.*, Phys. Rev. Lett. **147B**, 385 (1984).

<sup>6</sup>G. Barbiellini *et al.*, Phys. Rev. **39B**, 663 (1972).

<sup>7</sup>V. Bartenev *et al.*, Phys. Rev. Lett. **31**, 1088 (1973).

<sup>8</sup>U. Amaldi *et al.*, Phys. Lett. **66B**, 390 (1977).

<sup>9</sup>L. Baksay *et al.*, Nucl. Phys. **B141**, 1 (1978).

<sup>10</sup>N. Amos *et al.*, Nucl. Instrum. Methods Phys. Res., Sect. A **252**, 263 (1986).

<sup>11</sup>N. Amos *et al.*, Northwestern University Internal Report No. 101, 1981 (unpublished).

<sup>12</sup>D. Favart *et al.*, Phys. Rev. Lett. **47**, 1191 (1981).

<sup>13</sup>G. B. West and D. R. Yennie, Phys. Rev. **172**, 1413 (1968).

<sup>14</sup>R. N. Cahn, Z. Phys. C **15**, 253 (1982).